Large scale direct dynamic contact line simulations

S. Afkhami
Dept. Mathematical Sciences
New Jersey Institute of Technology

S. Zaleski and S. Popinet
Sorbonne Université, Centre National de la Recherche Scientifique,
Institut Jean le Rond ∂'Alembert, F-75005, Paris, France

Workshop on Modeling and Simulation of Interface Dynamics in Fluids/Solids and Applications, IMS 2018

Contact angle

[Ann. Rev. Fluid Mech., 45:269-292]

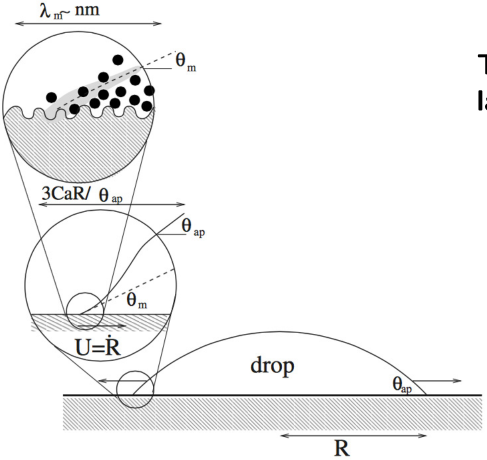

$$\theta_m = \cos^{-1}\left(\frac{\gamma_{sg} - \gamma_{sl}}{\gamma}\right)$$

There are two main challenges in large scale contact line modeling:

- to describe flow close to contact line
- to match hydrodynamic part of the problem to a microscopic neighborhood of contact line

Breakup of liquid filaments

No-Breakup Simulations

Breakup Simulations

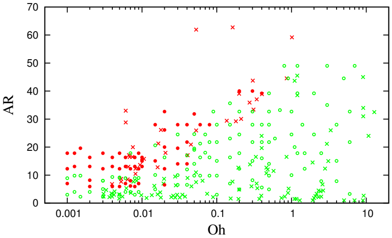

$\mathrm{Oh} = \frac{\mu}{\sqrt{\rho \sigma R_0}}$, experimental data from [Pita et al. PRL, 2012]

Afkhami et al., submitted: EPJ, 2018

Contact line phenomena in complex flows

Increasing in length, $2L_0 \approx 9$ mm, 11 mm, 15 mm and 17 mm from bottom to top. Oh ≈ 17, $R_0 \approx 0.17$ mm.

Afkhami et al., submitted: EPJ, 2018

Contact line phenomena in complex flows

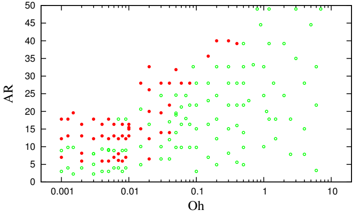

$\lambda = 1$

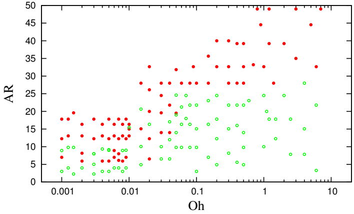

$\lambda = 0.1$

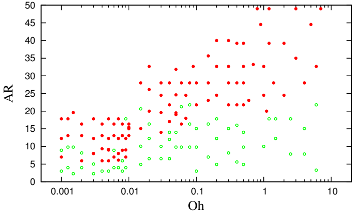

$\lambda = 0.01$

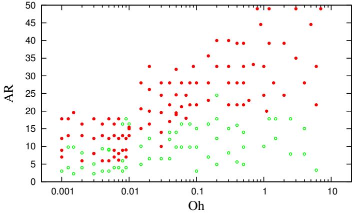

$\lambda = 0$

▸ No-Breakup Simulations Afkhami et al., submitted: EPJ, 2018

Pulse laser induced dewetting

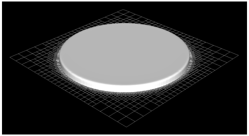

Cu: $h_0 = 15\text{Å}$, $R_0 = 150\text{Å}$

▸ $\theta_{eq} = 80^\circ$	▸ $\theta_{eq} = 115^\circ$	▸ $\theta_{eq} = 130^\circ$
time 70ps	80ps	90ps
ejection velocity 0	0	119 m s^{-1}

[Afkhami and Kondic, Phys. Rev. Lett., 2013]

Contact line phenomena in complex flows

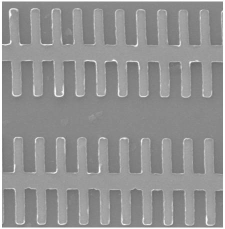

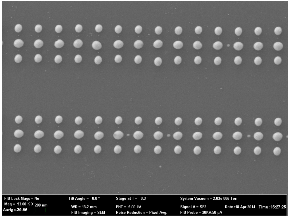

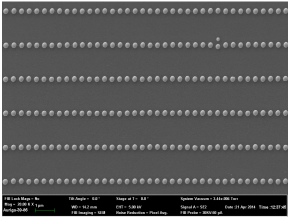

▸ Square-Wave-Simulations

Mahady et al., Phys. Fluids, 2015

Dewetting of thin films due to van der Waals force

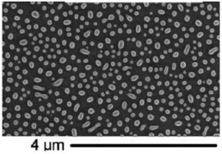

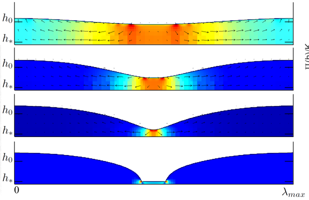

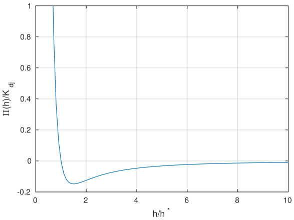

Break up of a perturbed thin film, $\lambda_{max} = 2\pi/k_{max}$

Dispersion relation of linearized equation with wavenumber k and growth rate ω:

$$\mu\omega/\gamma = -\frac{h_o^3}{3}\left[k^4 + k^2\Pi'(h_o)\right]$$

$$\Pi'(h_o) = \mathcal{K}_{dj}\left[m\left(\frac{h^*}{h_0}\right)^m - n\left(\frac{h^*}{h_0}\right)^n\right],\ \mathcal{K}_{dj} = \frac{\gamma(\cos\theta_{eq}-1)}{h^*}\frac{(m-1)(n-1)}{(m-n)}$$

Contact angle

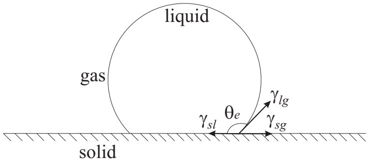

Equilibrium contact angle

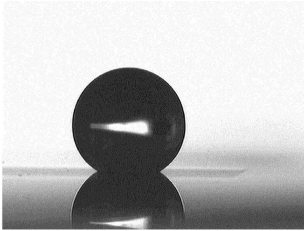

For a static contact line, Young's relation holds:

$$\gamma \cos \theta_e = \gamma_{sg} - \gamma_{sl}$$

Energy difference between wet and dry state - spreading parameter:

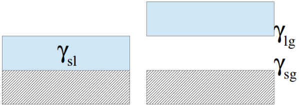

$$S_{eq} = \gamma_{sg} - (\gamma_{sl} + \gamma) = \gamma(\cos \theta_{eq} - 1)$$

Gerris: [An accurate adaptive solver for surface-tension-driven interfacial flows, S. Popinet J. Comput. Phys., 2009.]

The volume of fluid method:

- $\nabla \cdot \mathbf{u} = 0$
- $\rho(\frac{\partial \mathbf{u}}{\partial t} + \nabla \cdot \mathbf{u}\mathbf{u}) = -\nabla p + \nabla \cdot \tau + \mathbf{F}$

$$\tau = \mu \left(\nabla \mathbf{u} + \nabla \mathbf{u}^{\top} \right)$$

$$\mathbf{F}_{st} = \sigma \kappa \delta_s \hat{\mathbf{n}}$$

$$\delta_s \hat{\mathbf{n}} \approx \nabla f$$

$$\mathbf{F}_g = -\rho g \hat{y} = -\nabla(\rho(f) g y) + g y \nabla(\rho(f))$$

$$\mathbf{F}_{vdW} = -\nabla \phi_i$$

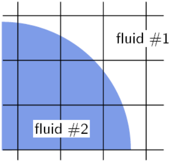

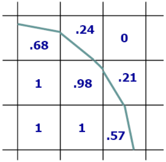

$$f_{i,j,k} = \frac{1}{\Omega_{i,j,k}} \int_{\Omega_{i,j,k}} f \, d\Omega$$

$$\frac{\partial f}{\partial t} + \nabla \cdot (\mathbf{u} f) = 0$$

$$\rho(f) = \rho_1 - (\rho_1 - \rho_2) f$$

$$\mu(f) = \mu_1 - (\mu_1 - \mu_2) f$$

Height-Function method: arbitrary contact angle

included:

- an implicit (numerical) slip at the grid scale
- well-defined static contact angle

not included:

- dynamic angle model
- microscopic physics: numerics is the microscopic physics

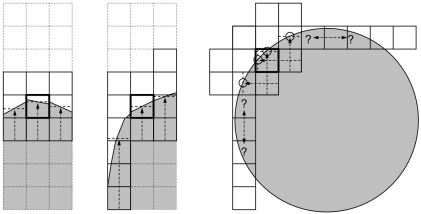

$$\kappa = \frac{h_{xx}}{(1+h_x^2)^{3/2}}, \qquad \mathbf{n} = (h_x, -1)$$

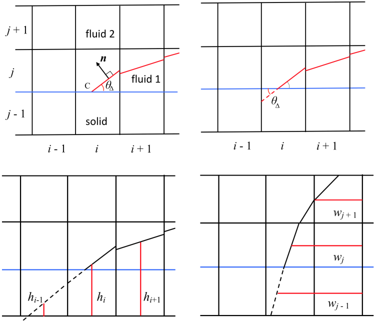

[Transition in a numerical model of contact line dynamics and forced dewetting, S. Afkhami, J. Buongiorno, A. Guion, S. Popinet, R. Scardovelli, and S. Zaleski, under revision, Journal of Computational Physics, 2018.]

Fluid/fluid/solid interactions

Potential (repulsive-attractive) on particle of phase i per unit volume of solid

$$\phi_i(r) = \rho_s \mathcal{K}_{is} \left(\left(\frac{\sigma_{is}}{r} \right)^p - \left(\frac{\sigma_{is}}{r} \right)^q \right)$$

$(p, q) = (12, 6)$
$i =$ vapor,liquid
ρ_s : particles density in solid
σ_{is} : length scale determining minimum potential
$\mathcal{K}_{is}$: particle interaction strength
$r = \sqrt{(x_0 - x_s)^2 + (y_0 - y_s)^2 + (z_0 - z_s)^2}$

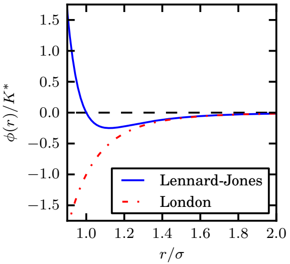

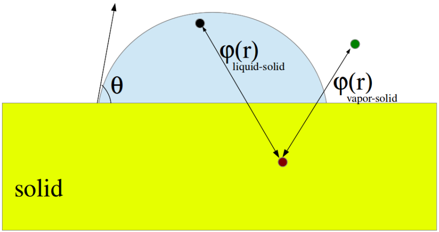

$$\phi_i(y) = \int_{-\infty}^{0} \int_{-\infty}^{\infty} \int_{-\infty}^{\infty} \phi_i(\mathbf{x}_0) dx_s dz_s dy_s$$

$$\phi_i(y) = \int_{-\infty}^{0}\int_{-\infty}^{\infty}\int_{-\infty}^{\infty} \phi_i(\mathbf{x}_0)\, dx_s dz_s dy_s =$$

$$2\pi\rho_s \mathcal{K}_{is}\sigma_{is}^3 \left(\frac{1}{(p-2)(p-3)} \left(\frac{\sigma_{is}}{y}\right)^{p-3} - \frac{1}{(q-2)(q-3)} \left(\frac{\sigma_{is}}{y}\right)^{q-3} \right)$$

where y is the height of the particle above the solid substrate.

$$\phi_i(y) = K_{is}\left(\left(\frac{h_i^*}{y}\right)^m - \left(\frac{h_i^*}{y}\right)^n \right)$$

where $m = p - 3$, $n = q - 3$, and

$$h_i^* = \left(\frac{(q-2)(q-3)}{(p-2)(p-3)} \right)^{\frac{1}{p-q}} \sigma$$

$$K_{is} = 2\pi\rho_s\rho_l\mathcal{K}_{is}h_i^* \frac{((p-2)(p-3))^{\frac{q}{p-q}}}{((q-2)(q-3))^{\frac{p}{p-q}}}$$

Lennard-Jones and contact angles

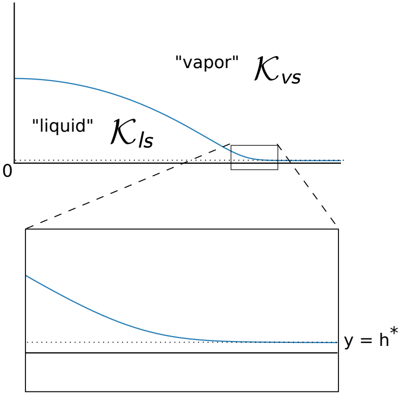

we refer to h^* as the precursor film thickness

Recall spreading parameter:

$$S_{eq} = \gamma_{sg} - (\gamma_{sl} + \gamma) = \gamma(\cos\theta_{eq} - 1)$$

Energy difference between wet and dry state:

$$\Delta E = \int_{\delta_0}^{\infty} (\phi_{vs} - \phi_{ls}) dy = S_{eq}$$

$$= (\mathcal{K}_{vs} - \mathcal{K}_{ls}) h^* \left[\frac{1}{m-1} \left(\frac{h^*}{\delta_0} \right)^{m-1} - \frac{1}{n-1} \left(\frac{h^*}{\delta_0} \right)^{n-1} \right]$$

Letting $\delta_0 = h^*$:

$$\mathcal{K}_{vs} - \mathcal{K}_{ls} = \frac{\gamma(1 - \cos\theta_{eq})}{h^*} \frac{(m-1)(n-1)}{(m-n)}$$

Volume-of-Fluid based Navier-Stokes solver

Method I: Body Force Formulation

$$\rho\left(\partial_t \mathbf{u} + \mathbf{u}\cdot\nabla\mathbf{u}\right) =$$

$$-\nabla p + \nabla\cdot\tilde{\tau} + \gamma\kappa\delta_s\mathbf{n} + \mathbf{F}_B(\mathbf{x})$$

$$\mathbf{F}_B(\mathbf{x}) = -\nabla(\phi_i(y))$$

$$\mathbf{F}_B(\mathbf{x}) = \left[f\mathcal{K}_{ls} + (1-f)\mathcal{K}_{vs}\right]\nabla(\phi_i(y))$$

Method II: Balanced Pressure Formulation

$$\rho\left(\partial_t \mathbf{u} + \mathbf{u}\cdot\nabla\mathbf{u}\right) =$$

$$-\nabla p^* + \nabla\cdot\tilde{\tau} + \gamma\left(\kappa - \frac{\mathcal{K}\phi_i(y)}{\gamma}\right)\delta_s\mathbf{n}$$

$$\mathcal{K} = \mathcal{K}_{ls} - \mathcal{K}_{vs}$$

$$p^* = p + \left[f\mathcal{K}_{ls} + (1-f)\mathcal{K}_{vs}\right]\left[-\phi_i(y)\right]$$

$$\phi_i(y) = \mathcal{K}_{is}\left[\left(\frac{h^*}{y}\right)^m - \left(\frac{h^*}{y}\right)^m\right],\ \mathcal{K}_{vs} - \mathcal{K}_{ls} = \frac{\gamma(1-\cos\theta_{eq})}{h^*}\frac{(m-1)(n-1)}{(m-n)}$$

The discrete approximation of $\mathbf{F}_B(\mathbf{x})$ and $\mathcal{K}\phi_i(y)$ are implemented in GERRIS (freely available at gfs.sf.net). [Mahady et al., JCP, 2015]

Contact Angles, $\theta_i = \theta_{eq}$, $\gamma = \mu = \rho = 1$

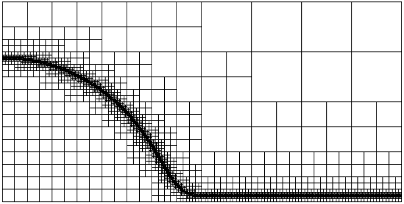

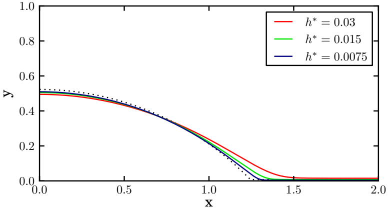

$\theta_{eq} = \pi/4$

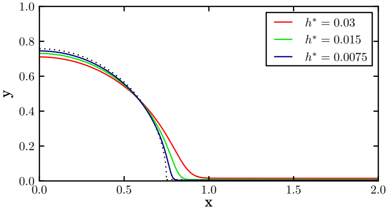

$\theta_{eq} = \pi/2$

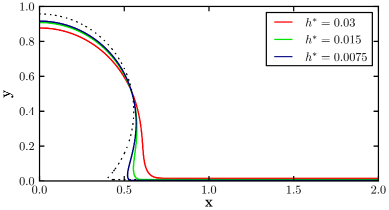

$\theta_{eq} = 3\pi/4$

Spinodal dewetting: 3D results, liquid copper, $\theta_{\text{eq}} = 0.439\pi, \quad \text{Oh} = 0.487$

Simulation | Simulation

4*nm* thick | 8*nm* thick

Nonlinear film breakup: 3D results

$$h(t=0,x,z) = h_0 + \zeta(x,z),$$
$$\zeta(x,y) = \sum_{i=1}^{30} \sum_{j=1}^{30} \delta_{ij} \cos\left(\frac{2\pi x}{\lambda_i}\right) \cos\left(\frac{2\pi z}{\lambda_j}\right),$$

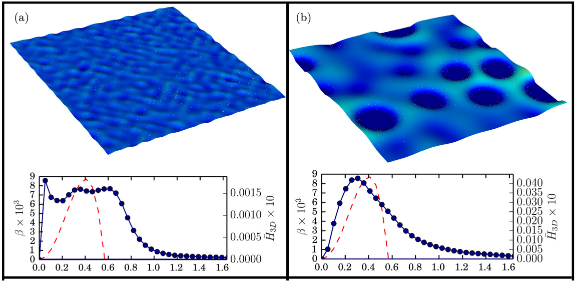

$$\bar{H}_{3D}(t,k) = \frac{1}{N_s} \sum_{j=1}^{N_s} \frac{1}{2}\left(\hat{H}_j(t,k,0) + \hat{H}_j(t,0,k)\right).$$

Spinodal dewetting: 3D results, liquid copper, $\theta_{\text{eq}} = 0.439\pi, \quad \text{Oh} = 0.487$

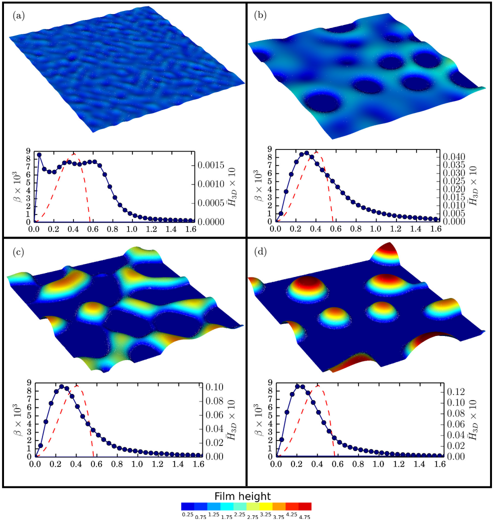

[Mahady et al., PoF, 2016]

Spinodal dewetting: 2D vs 3D results, $\mathrm{Oh} = \mu/\sqrt{\gamma\rho L} = 0.48$

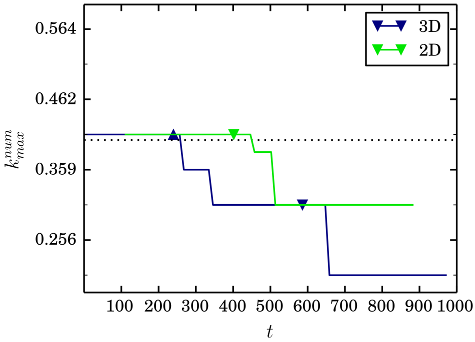

Dewetting transition: Landau–Levich–Derjaguin film

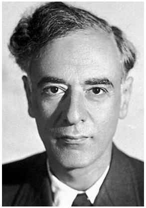

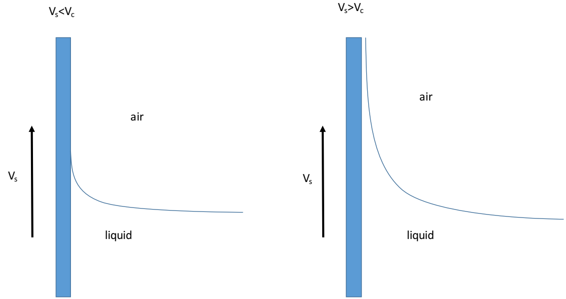

Levich and Landau (1942). Acta Physicochimica
Derjaguin (1943). Acta Physicochimica

Dewetting transition: Landau–Levich–Derjaguin film

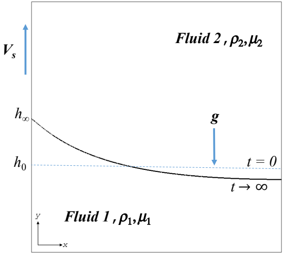

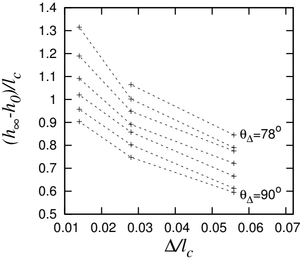

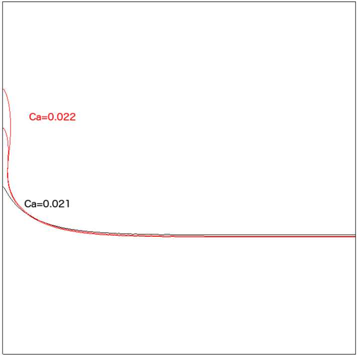

Can we numerically predict the transition?

$$\mathrm{Ca} = \mu_1 V_s/\sigma = 0.04$$

Is this transition universal?

$$l_c = \sqrt{\sigma/[(\rho_1 - \rho_2)g]}$$

Motivation: nucleate boiling, microlayer formation

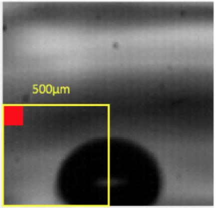

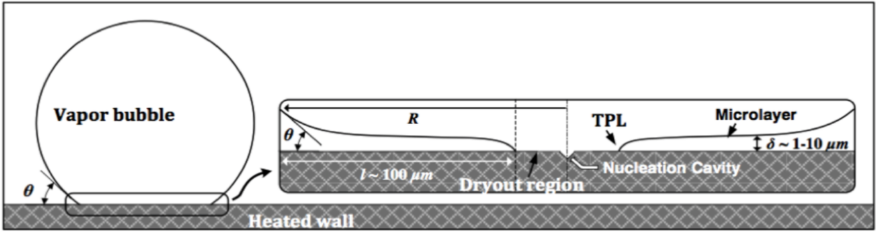

[A. Guion, S. Afkhami, S. Zaleski and J. Buongiorno, under revision, IJHMT]

Lubrication approximations, $\theta_e \to 0$

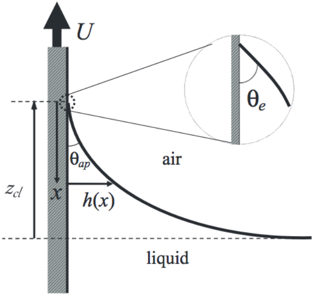

inner region: $$\frac{\partial^3 h}{\partial x^3} = \frac{3\mathrm{Ca}}{(h^2 + 3\lambda h)}$$

λ is slip length

outer region: $\kappa = z_{cl} - x$

$$\mathrm{Ca}_{cr} = (\theta_e^3/9)\left[\ln\left(\frac{[\mathrm{Ca}_{cr}]^{1/3}\theta_e}{18^{1/3}\pi[\mathrm{Ai}(S_{\max})]^2\sqrt{2}\lambda}\right)\right]^{-1}$$

$$\theta_{app} \to 0, \kappa = \sqrt{2}$$

[Chan, Snoeijer, Eggers, Phys. Fluids 24 (2012).]

Hydrodynamic theories of the dynamic contact line and the dewetting transition; Cox's theory [R. G. Cox, JFM 1986].

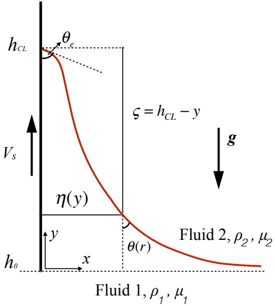

$$G[\theta(r)] = G(\theta_e) - \mathrm{Ca}\ln(r/\lambda) - \mathrm{Ca}\frac{Q_i}{f(\theta_e, q)} + o(\mathrm{Ca})$$

$$G[\theta(r)] = G(\theta_e) - \mathrm{Ca}\ln(r/\lambda \exp[\frac{f(\theta_e, q)}{Q_i}]) + o(\mathrm{Ca})$$

$\lambda \to \Delta$, $\theta_e \to \theta_\Delta$ and $\phi(\theta_\Delta) = \exp[-\frac{f(\theta_\Delta, q)}{Q_i}]$

$$\theta(r) = G^{-1}\left[G(\theta_\Delta) - \mathrm{Ca}\ln(r/(\Delta/\phi))\right] + o(\mathrm{Ca})$$

$$\phi(\theta_\Delta) = \frac{\Delta}{r}\exp[\frac{G(\theta_\Delta) - G[\theta(r)]}{\mathrm{Ca}}]$$

$$\theta(r)|_{\mathrm{Ca}_{cr}} \to 0 \Rightarrow \phi(\theta_\Delta) = \frac{\pi \mathrm{Ai}^2(s_{\max})}{3^{1/3}2^{-5/6}} \frac{\Delta}{\mathrm{Ca}_{cr}^{1/3} l_c} \exp\left[\frac{G(\theta_\Delta)}{\mathrm{Ca}_{cr}}\right]$$

Accuracy of Direct Dynamic Contact Line Simulations Near the Forced Dewetting Transition

- A distinguished feature of proposed numerical model is consideration of large contact angles ($\geq 90^\circ$) and arbitrary viscosity ratios, in contrast to available asymptotic models.
- First time showing logarithmic dependence of interface slope on distance to contact line using direct numerical simulations.
- First time characterizing the implicit numerical slip length.
- Results (probably) depend on the exact numerical method used.

Numerical setup

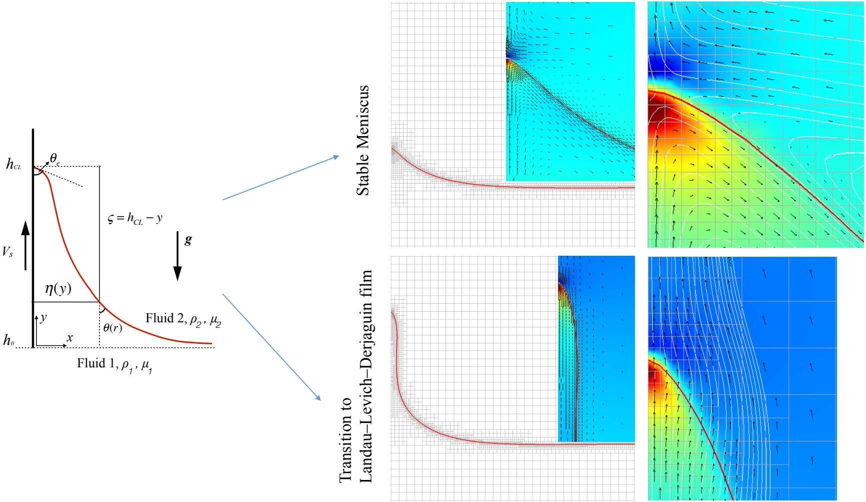

$0.0008 \leq \mathrm{Ca} = \mu_1 V_s/\sigma \leq 0.2$

$15^\circ \leq \theta \leq 110^\circ$

$l_c = \sqrt{\sigma/[(\rho_1 - \rho_2)g]} \approx L/10$, l_c of water/air ~ 2 mm

$1/256 \leq l_c/\Delta \leq 1/32$

Results

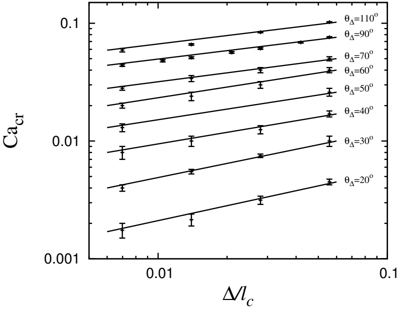

Ca_cr
Δ/l_c
0.1
0.01
0.001
0.01
0.1
θ_Δ=110°
θ_Δ=90°
θ_Δ=70°
θ_Δ=60°
θ_Δ=50°
θ_Δ=40°
θ_Δ=30°
θ_Δ=20°

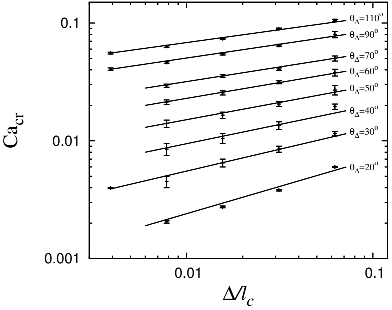

Ca_cr
Δ/l_c
0.1
0.01
0.001
0.01
0.1
θ_Δ=110°
θ_Δ=90°
θ_Δ=70°
θ_Δ=60°
θ_Δ=50°
θ_Δ=40°
θ_Δ=30°
θ_Δ=20°

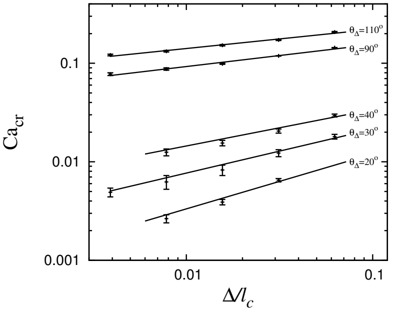

Ca_cr
Δ/l_c
0.1
0.01
0.001
0.01
0.1
θ_Δ=110°
θ_Δ=90°
θ_Δ=40°
θ_Δ=30°
θ_Δ=20°

Numerical verification of the theory of Cox

$$\theta(r) = G^{-1}\left[G(\theta_\Delta) - \mathrm{Ca}\ln(r/(\Delta/\phi))\right], \quad q = 1, \quad \theta_\Delta = 110^\circ$$

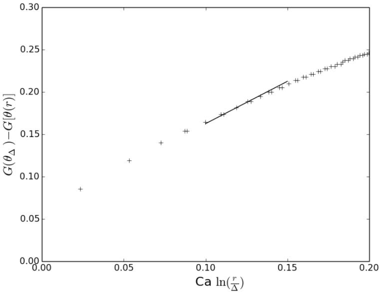

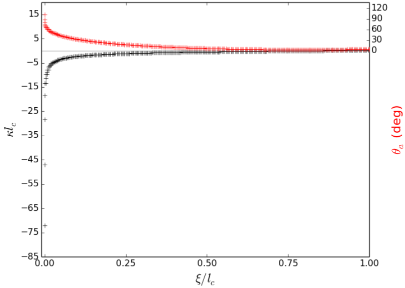

$$\phi = 2.94, \Delta/l_c = 0.004, \mathrm{Ca} = 0.058$$

Numerical verification of the theory of Cox

$$\theta(r) = G^{-1}\left[G(\theta_\Delta) - \mathrm{Ca}\ln(r/(\Delta/\phi))\right], \quad q = 1, \quad \theta_\Delta = 110^\circ$$

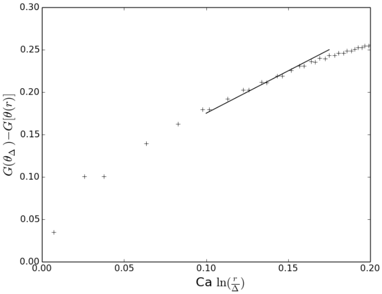

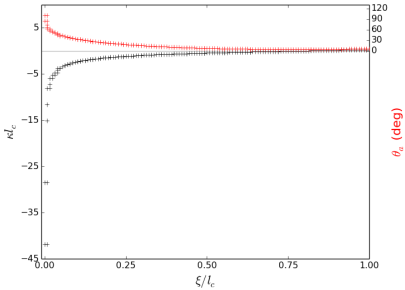

$$\phi = 3.22, \Delta/l_c = 0.008, \mathrm{Ca} = 0.064$$

Numerical verification of the theory of Cox

$$\theta(r) = G^{-1}\left[G(\theta_\Delta) - \mathrm{Ca}\ln(r/(\Delta/\phi))\right], \quad q = 1, \quad \theta_\Delta = 110^\circ$$

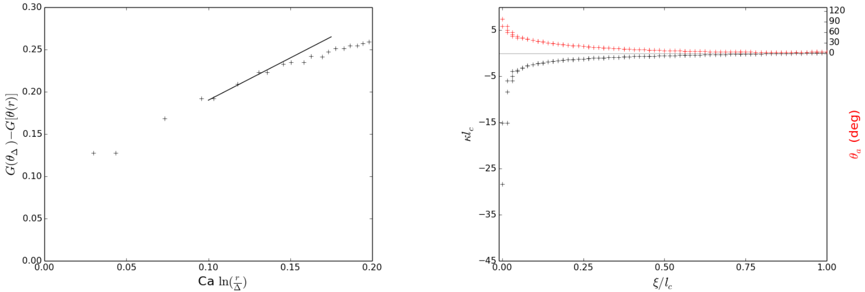

$$\phi = 3.37, \Delta/l_c = 0.016, \mathrm{Ca} = 0.074$$

Numerical verification of the theory of Cox

$$\theta(r) = G^{-1}\left[G(\theta_\Delta) - \mathrm{Ca}\ln(r/(\Delta/\phi))\right], \quad q = 0.02, \quad \theta_\Delta = 90^\circ$$

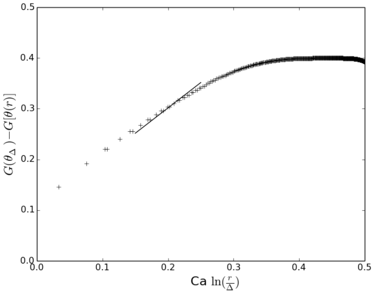

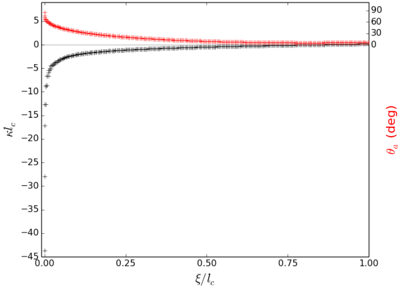

$$\phi = 3.42, \Delta/l_c = 0.004, \mathrm{Ca} = 0.08$$

Numerical verification of the theory of Cox

$$\theta(r) = G^{-1}\left[G(\theta_\Delta) - \mathrm{Ca}\ln(r/(\Delta/\phi))\right], \quad q = 0.02, \quad \theta_\Delta = 90^\circ$$

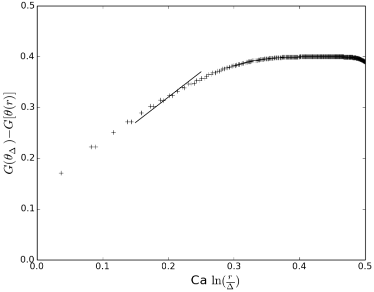

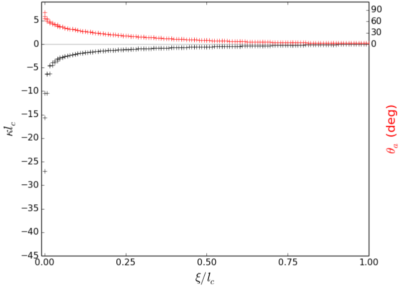

$$\phi = 3.79, \Delta/l_c = 0.008, \mathrm{Ca} = 0.09$$

Numerical verification of the theory of Cox

$$\theta(r) = G^{-1}\left[G(\theta_\Delta) - \mathrm{Ca}\ln(r/(\Delta/\phi))\right], \quad q = 0.02, \quad \theta_\Delta = 90^\circ$$

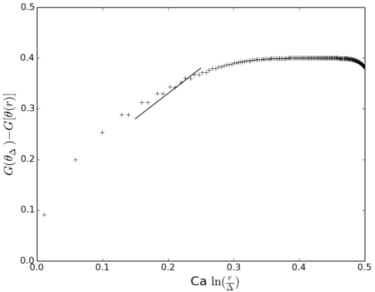

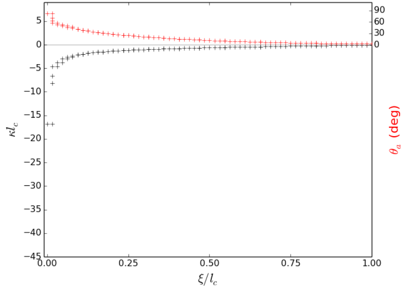

$$\phi = 3.67, \Delta/l_c = 0.016, \mathrm{Ca} = 0.1$$

Numerical verification of the theory of Cox

$$\theta(r) = G^{-1}\left[G(\theta_\Delta) - \mathrm{Ca}\ln(r/(\Delta/\phi))\right], \quad q = 1, \quad \theta_\Delta = 40^\circ$$

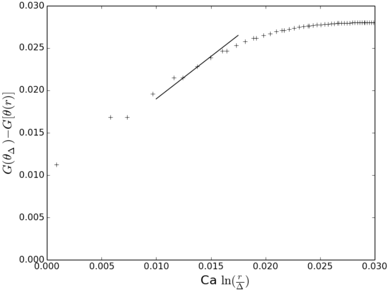

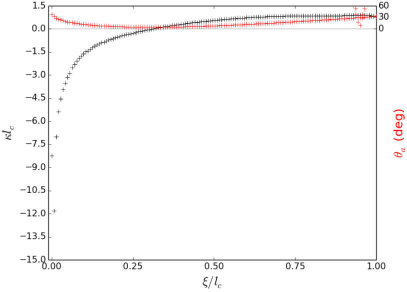

$$\phi = 2.42, \Delta/l_c = 0.008, \mathrm{Ca} = 0.008$$

Numerical verification of the theory of Cox

$$\theta(r) = G^{-1}\left[G(\theta_\Delta) - \mathrm{Ca}\ln(r/(\Delta/\phi))\right], \quad q = 0.02, \quad \theta_\Delta = 40^\circ$$

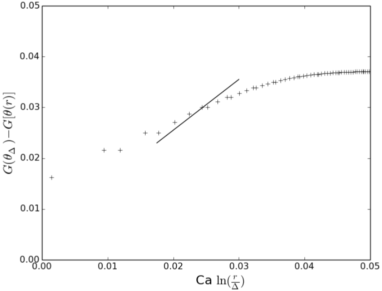

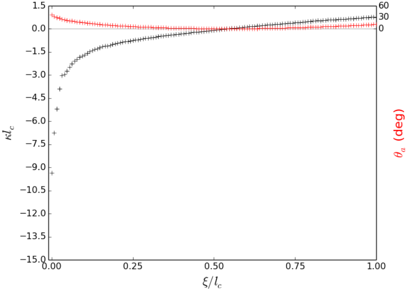

$$\phi = 1.53, \Delta/l_c = 0.008, \mathrm{Ca} = 0.013$$

Numerical verification of the theory of Cox

$$\mathrm{Ca}_{cr} = (\theta_e^3/9)\left[\ln\left(\frac{[\mathrm{Ca}_{cr}]^{1/3}\theta_e}{18^{1/3}\pi[\mathrm{Ai}(S_{\max})]^2\sqrt{2}\lambda}\right)\right]^{-1}$$

$$\phi(\theta_e) = \frac{\pi \mathrm{Ai}^2(s_{\max})}{3^{1/3}2^{-5/6}}\frac{\lambda}{\mathrm{Ca}_{cr}^{1/3} l_c}\exp\left[\frac{\theta_e^3/9}{\mathrm{Ca}_{cr}}\right]$$

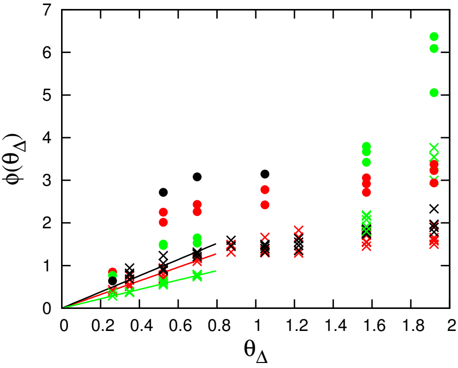

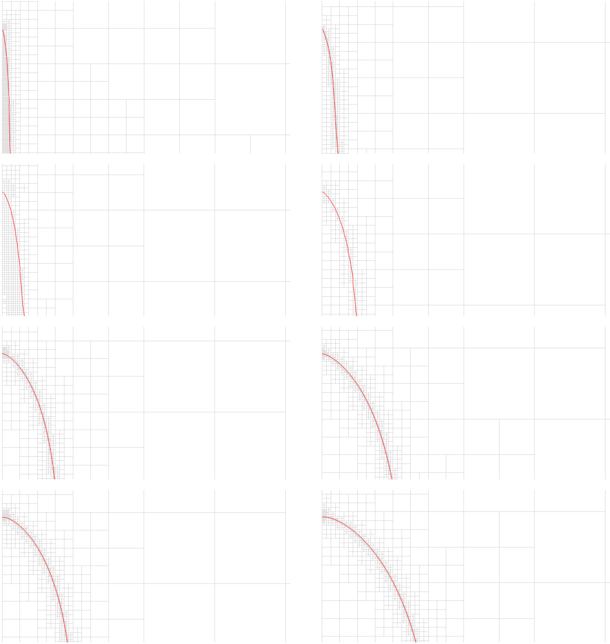

Conclusions

- The results serve as an indirect verification of the Cox theory.
- Our numerical procedure can be thought of as a way to achieve mesh independent contact line simulations.
- Future work: extend the study to various scenarios, such as drop spreading, micro-layer formation, etc., to confirm the universality of the numerical procedure.

Asymptotic matching solution

R. G. Cox [JFM (1986)]:

$$G(\theta_{out}) = G(\theta_{in}) + \mathrm{Ca}\ln(\varepsilon^{-1}) + O(\mathrm{Ca})$$

$$G(\theta) = \int_0^\theta \frac{d\theta'}{f(\theta', q)},$$

$$f(\theta, q) =$$

$$\frac{2\sin\theta\{q^2(\theta^2 - \sin^2\theta) + 2q[\theta(\pi-\theta) + \sin^2\theta] + [(\pi-\theta)^2 - \sin^2\theta]\}}{q(\theta^2 - \sin^2\theta)[(\pi-\theta) + \cos\theta\sin\theta] + [(\pi-\theta)^2 - \sin^2\theta](\theta - \cos\theta\sin\theta)}$$

- As $\mathrm{Ca}, \varepsilon \to 0$, $\theta_{out} \to \theta_{in}$ if $\mathrm{Ca}\ln(\varepsilon^{-1}) \to 0$.
- $\varepsilon = r_m/r$ is not uniquely defined.
- Effect of corresponding small scales can be summarized with θ_{in} and the microscopic length scale r_m.